Geomorphological Approach In Active Tectonics For The Cartography Of Landslide And Rock Fall Hazards In The North-West Part Of The Region Of Yaounde-Cameroon

Roger BISSAYA [1,4*], Richard Tanwi GHOGOMU[1,2], Serge Martial AKISSEBINI [1,3], Bernard NJOM [1], Eric Lamine GOMSSI [1,3], Nguo Sylvestre KANOUO [2]

[1] Department of Earth Sciences, University of Yaounde I, Cameroon
[2] Faculty of Mines and Petroleum Industries, University of Maroua, Cameroon
[3] CRESA Forêt-Bois, Faculty of Agronomy and Agricultural Sciences, University of Dschang, Cameroon
[4] School of Engineering and Science, Atlantic International University, USA
Corresponding Author: Roger Bissaya

Résumé
Le secteur Nord-Ouest de la région de Yaoundé, localisé dans la zone mobile d'Afrique centrale, recèle les marques de la tectonique ductile datée 600 ± 20 Ma ; et celles de la tectonique cassante datant de 600 ± 20 Ma à l'actuel. La tectonique active suivant la faille de la Sanaga est considérable. La distribution des vestiges de glissements de terrain et d'éboulements suivant les configurations et reconfigurations spatiales des grands accidents structuraux révèle un guidage tectonique. En utilisant une approche géomorphologique dans ce contexte de tectonique active, par la superposition des éléments pétro-structuraux aux discontinuités géomorphologiques, il a été établi une carte de l'aléa plus rapproché de la réalité du terrain révélant un « aléa très fort » dans trois linéaments majeurs orientés SSW-NNE et E-W ; et un « aléa fort à moyen » dans deux linéaments intermédiaires orientés WSW-ENE.
Mots-clés : glissements de terrain, éboulements, éléments structuraux, géomorphologie, région de Yaoundé.
---ABSTRACT---
The North-West sector of Yaounde, located within the mobile belt of Central Africa reveals imprints of ductile tectonics dating from 600 ± 20 Ma; and those of fracturing tectonics dating from 600 ± 20 Ma to present. The active tectonics along the Sanaga fault is very remarkable. The distribution of marks of landslides and rocks falls along the spatial configurations and reconfigurations of great structural accidents reveals a tectonic guide. In using a geomorphological approach in this active tectonic context, by the superposition of petro-structural elements to geomorphological discontinuities, it was the establishment of a map of the considered field which is more close to the field reality. It reveals a "very high" hazard in three major lineation oriented towards SSW-NNE and E-W; and a "high to average" hazard in two intermediate lineation oriented WSW-ENE.
KEYWORDS: landslide, rock fall, structural elements, geomorphology, Yaounde region.

I.   INTRODUCTION

The North-West sector of the Yaounde region which can be artificially located between latitudes 3°45' (3,75°) and 4°00' (4,00°) North, and longitudes 11°20' (11,33°) et 11°35' (11,67°) East (***Fig. 1***) is within an active tectonic context, due in part by its localisation of the Central African mobile belt [1] [2] still called North Equatorial Panafrican Chain [3] [4] or the Oubanguides Chain [5] [6], strongly affected by orogenesis issued from polyphased geodynamic activity comprising D_1, D_2, D_3 [7] [8] [9] and D_4[8] [9] ductile deformation events dating 600 ± 20 Ma [10] [9] [11] and brittle deformation events[3] [12] [13] [14] dating from 600 ± 20 Ma to present. Apart from this, other anthrompogenic action and scarped relief [15] [16] [17], the presence of great structural accident, their orientation, their redistribution across time and space, etc… influence also the spatial configuration of the hazard. On the other part, evidences of ancient and recent manifestation of landslide and rock fall seem to converge towards the distribution to tectonic guidage ; from where there is the necessity to revise the map of these hazards in this area. The present article will extend right to the end of the subject while synchronizing the field, library and laboratory data to obtain a thematic map more close to the field reality. The first step will consist of collecting and treating the field data and the field numerical model with the objective of vectorising the maps of primary information; the second step will consist of crossing the maps of primary information with the perspective to generate a synthetic map.
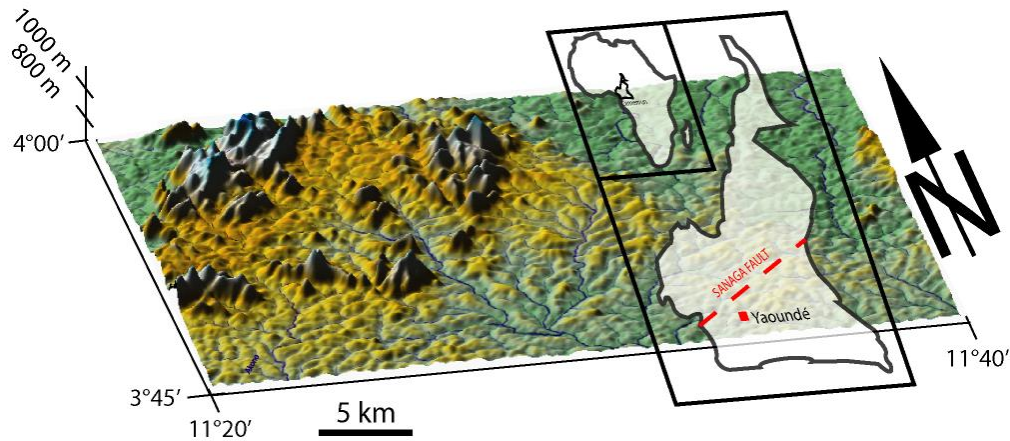
Figure 1 : Bloc diagram of the study area

1.   Material and methods of research
1.1.   Natural milieu
1.1.1.   Climate

Precipitation results from meteoric water that falls on the earth's surface in the form of a liquid (rain or dew) and more rarely in the solid form (hailstone). The registered data shows that the amount of rainfall is higher (1562 mm/year averagely), August being the month of minimum atmospheric saturation (H = 84%) and February being that of maximum atmospheric saturation (H = 73%). The temperature fluctuates between 22.8°C and 25.47°C (*Table 1*). The precipitation histogram shows that the area is subjected to a Guinean equatorial climate having two dry seasons and two rainy seasons which are alternatively and of variable intensities (*Fig. 2 and Table 2*). However, the presence of rains all along the year holds a residual humidity at soils level.

Table 1 : Climatic data of the Yaounde region from 1981 to 2010 [18]

Month	Jan.	Feb.	Mar.	Apr.	May	June	July	Aug.	Sept.	Oct.	Nov.	Dec.	
P (mm)	21.27	47.59	139.0	178.8	207.8	158.4	71.5	89.0	227.0	282.2	114.7	24.5	Total 1562
H (%)	75	73	76	80	81	83	82	84	82	82	80	79	Moy. 79,2
T (°C)	24.5	25.47	25.1	24.6	24.3	23.5	22.8	22.8	23.3	23.4	23.9	23.9	Moy. 23.96

P : precipitation ; H : relativehumidity ; T : temperature
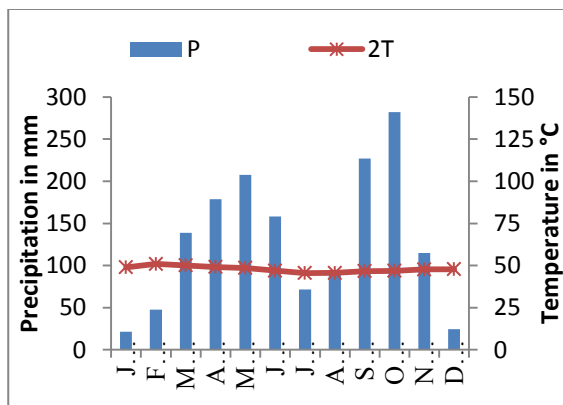
Figure 2 : Ombrothermic diagram applied to the data from 1981 to 2010 in Yaounde [18]

Table 2 : Annual distribution of seasons in Yaounde and its environs

Seasons	Periods
Short rainy season	March - june
Short dry season	July - August
Long rainy season	September - November
Long dry season	December - February

1.1.2.   Geomorphology

Geomorphological units are between 800 m and 1000 m above the sea level, covering about 40% of the surface. These units are made up of hills with very pointed tops and convex or convexo-concave slopes. They have very steep slopes and which attain sometimes 50% [**19**]. Their slopes are incised by very strainght and narrow walleys. The following tops corresponds to the belonging criteria to this group : Messebé (885 m), Minloua (888 m), Mvog-Betsi (902 m), Mbokdoum (953 m), Akokndoué (967 m), Bikariga (983 m).

The geomorphological units with heights above 1000 m cover about 15% of the surface. These units are generally having very large and tabular tops, with irregular contours. Their slopes are convex and steep toward the summit. The slopes are very teep and at times are more than 50% [19]. These massifs define morphology of rochy peaks [20]. The following tops holds the criteria of belonging to theirs group : Messa (1015 m), Nkolbissa (1031 m), Djokye (1042 m), Nkolmeyang (1072 m), Febe (1077 m), Ngoya (1082 m), Nkoloman (1086 m), Mbankolo (1098 m), Nkolobot (1105), Nkoabanaga (1123 m), Ngoa-ekele (1125 m), Eloumden (1209 m), Nkolondom (1221 m), Mbam-Minkom (1295 m).

1.1.3. Itinerary of the study sites

The preparatory stage for the field trips was the systematic identification of the "high reliefs" of the study area from the topographical map on sheet NA-32-XXIV, Yaounde 3d at 1/50 000 and on the sheet NA-32-XXIV, Yaounde 4c at the scale of 1/50000 [21] and on the satellite image in order to select the sites whose accessibility would allow a detailed study.

The first field trips were carried out to prospect the sites at Tsinga, Mvog-Betsi, Oliga, Messa, Akokndoue, Messebe, Nkolondom, Febe, MbamMinkom, Mbokdoum, Eloumden and Mvolye (*Fig. 3*).

.The second field trips were carried out to do a detailed study of the geological and environmental parameters of the selected sites. Only five of the twelve sites prospected were retained to be studied which are : Mvog-Betsi, Akokndoue, Oliga, Messa and Tsinga.

1.2. Observations and analysis made

1.2.1. Historical seismotectonic and instability of the slopes

1.2.1.1. Historical seismotectonic

It is the ductile tectonic context D_1, D_2 [7] [8] [9] dated 600 ± 20 Ma [10] [9] [11] that has configured the structures into domes and bassins in the katazone of the Yaounde region. Later the fracture tectonic context D_3 [3] [12] [13] [14] and D_4 [8] [9] and gave rise to shearing and collapsing structures which are in the origin of earthquakes. Numerous seismic manifestations have been recorded in Cameroon in the course of the 20th century within the Sanaga fault and theKribi –Tapare axis, crossing the Yaounde region, we can cite amongst others the following earthquakes : that of 1903 at Grand Batanga, 1911 at Lolodorf, 1913 at Akonolinga, 1945 at Ouesso, 1969 at Yoko, 1983 at Magha, 1987 at Tibati and at Kribi, 1987 at Tapare [22] [23] ; 2000 at Garoua Boulay and 2005 at Monatele (*Fig. 4*). Across the outcrops, the imprints of the said seismicity are abundant (*Photos 1a, 1b, 2, 3, 4 and 5*).

1.2.1.2. The history of instability of slopes

Numerous manifestations of quantity mass movements have been recorded within the study zone. We can cite amongst others the landslide of 1978 and 1983 at Nkol Bikok, 1990 at Oyom-Abang, 1998 at the Quarry of Messa ; the rock fall of April 2006 at Messebe [18]. Also, vestiges of recent and ancient manifestations such as gneissic sandstones, mesoscopic flows, fault mirrors, shearing joints that are averagely deep to superficial points to the frequency of this phenomenon (*Photos 6, 7, 8 and 9*).
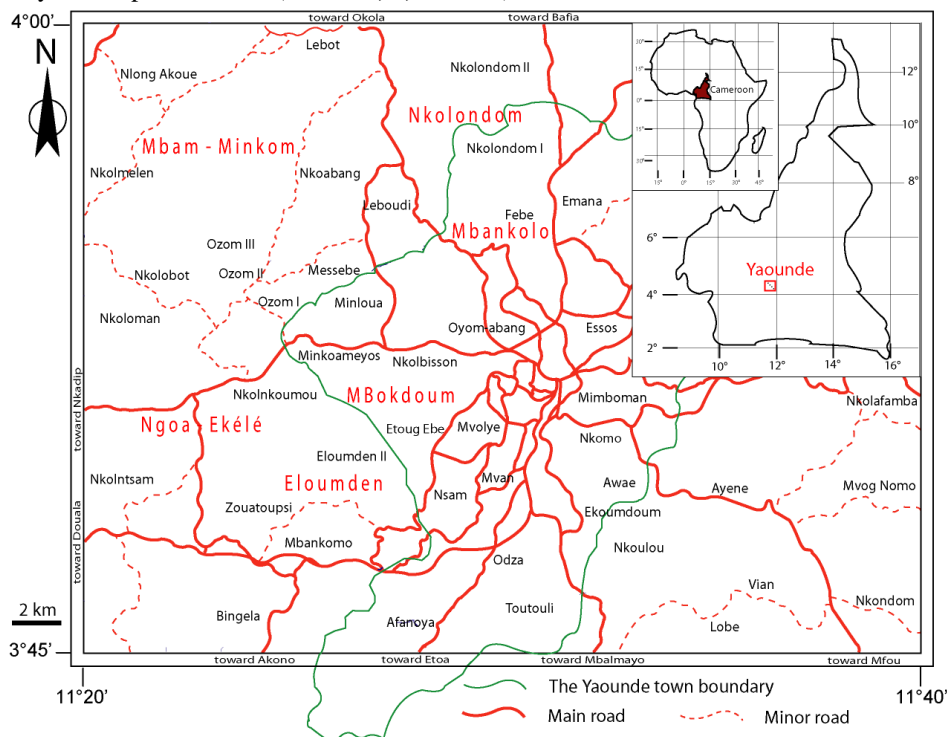

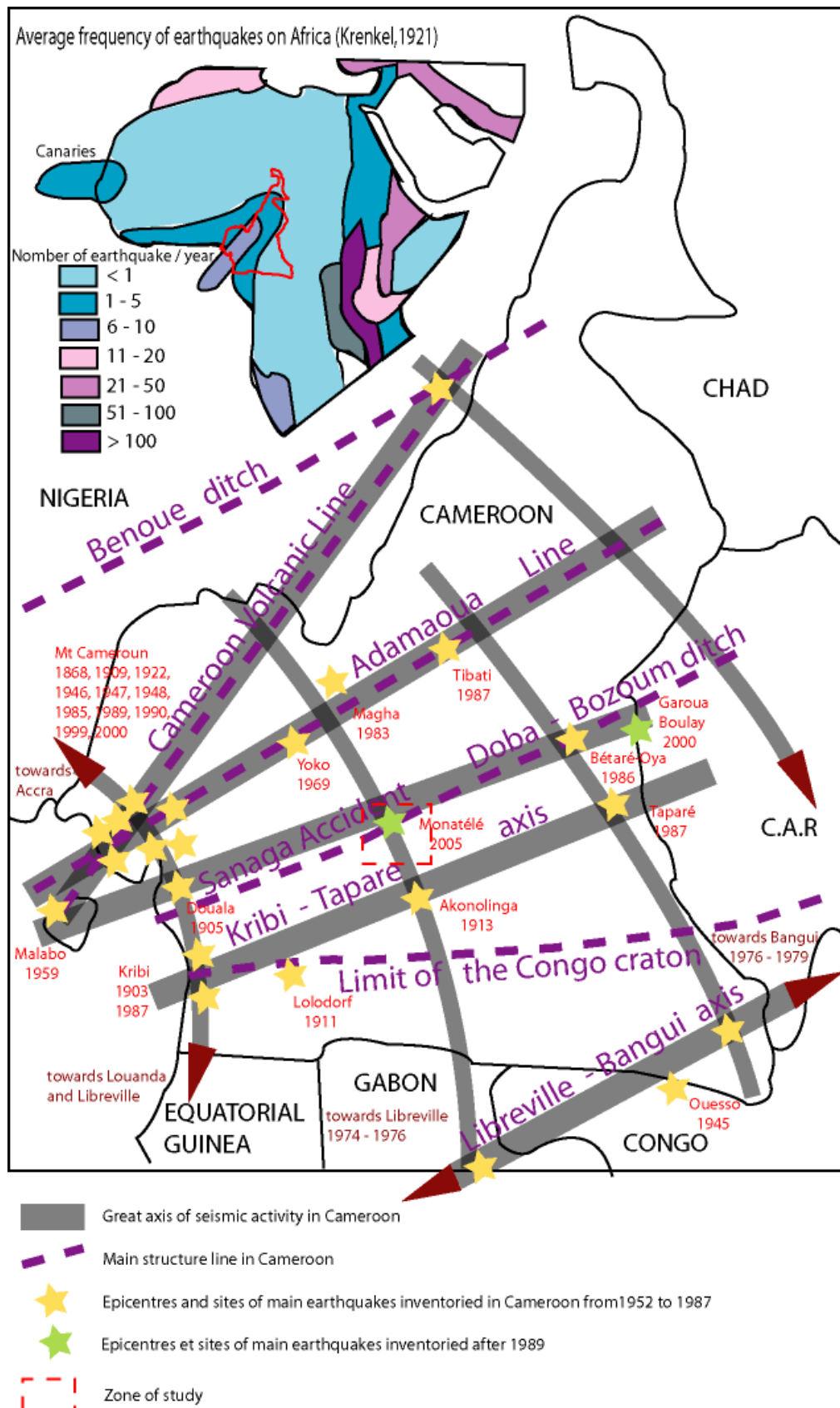**Figure 3 : Itinerary of study sites**

Figure 4 : Great axis of seismotectonic activity in Cameroon [22] and [23], modified by the addition of the after 1989 earthquake epicentres
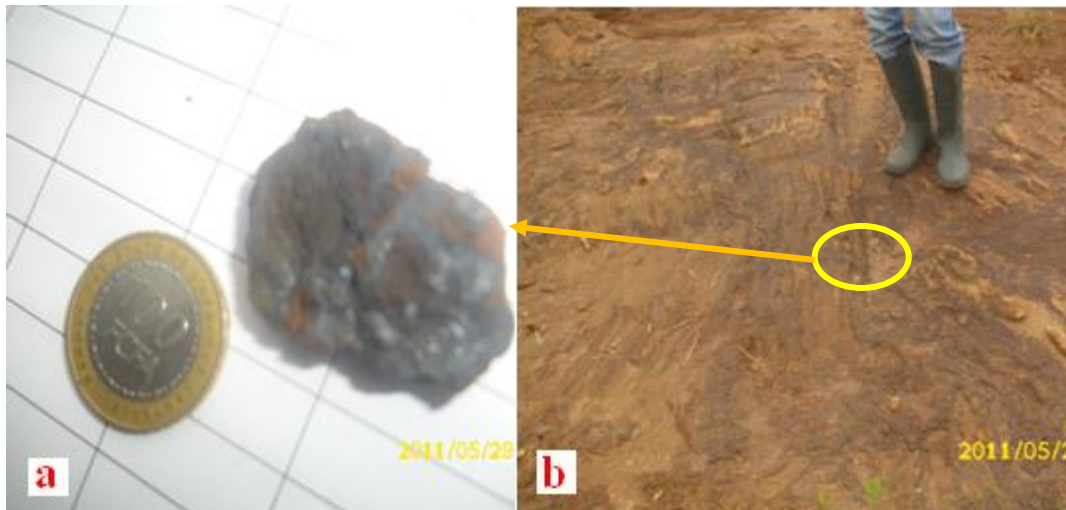
Photo 1 : Pseudotachylites (a), markers of the walls of earthquakes (b) at Minkoameyos [18]

Photo 2 : Cataclastic breccia encountered at Oliga[18]

Photo 3 : Horizontal mylonites at Mvog-Betsi (R = main rock) [14]

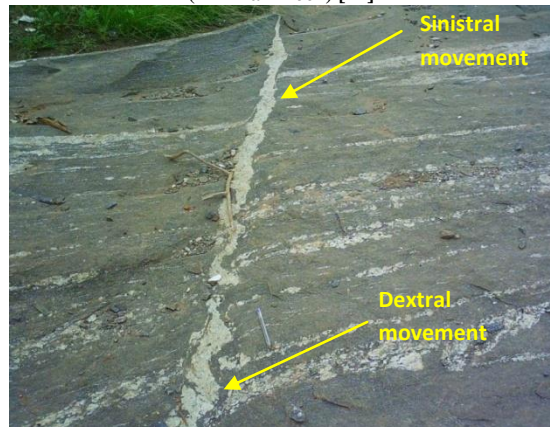**Photo 4 : Paraclase complex in the outcrop at Nkolbon [18]**

Photo 5 : Paraclase with double display (dextral and sinistral) in the Nkolbon outcrop [18]

Photo 6 : Quartzo-feldspathic filled joints, materializing an episode of brittle tectonic

Photo 7 : Mount Mbankolo (1098 m), and its fault planes
(Imagerie©2013, Ones/Spot image Digital globe)

Photo 8 : Mbankolo : dome of about 200 tons demobilized by recent throw or overthrow of the deep fractureof the milieu
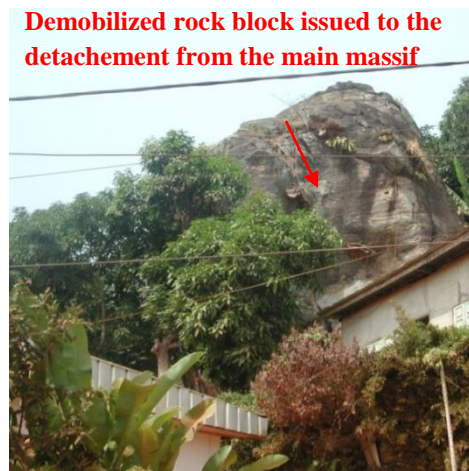
Photo 9 : Mvog-betsi : dome of about 300 tons demobilized by recent throw or overthrow of deep fracture of the milieu

1.2.2. Structural elements

1.2.2.1. Intense fracturation at a mesoscopic scale

At a mesoscopic scale, fracturation is marked by families of foliation planes (***Tables 3, 4, 5, and 6***), dry fissures and filled fissures (***Tables 7, 8, 9 and 10***). Maximum constraint is vertical, while intermediate and minimum constraint are subhorizontal (***Tables 11 and 12***). Generally, the distribution of these families of fractures designs the "Chocolate Tablets" across the outcrops (***Fig.5, 6, 7 and 8***).

From average spacing ($E_{tm} = \sum (E_{ti})(N_{ti}) / N$ [**24**] with : E_{tm} : average spacing, E_{ti} : measured along the t axis, N_{ti} : number of specific spacing measured along the t axis, N : total number of spacing measured) (***Table 13***) the conjecture of the average block is about 0,98 m^3 about (1,45 m x 1,30 m x 0,52 m).

Table 3 : Measurements taken on the subhorizontal fractures on the station at Cité-Verte
(position : N03°52'37,8'' ; E11°28'49,0'' ; H = 813 m) [25]

N°	Azimuth	Dip	N°	Azimuth	Dip	N°	Azimuth	Dip	N°	Azimuth	Dip
1	N358	16°	9	N284	25°	17	N264	10°	25	N288	08°
2	N000	07°	10	N300	27°	18	N280	16°	26	N292	07°
3	N180	10°	11	N320	15°	19	N030	09°	27	N286	20°
4	N002	64°	12	N320	16°	20	N230	10°	28	N000	03°
5	N025	15°	13	N280	30°	21	N090	07°	29	N276	14°
6	N290	12°	14	N276	34°	22	N164	10°	30	N020	07°
7	N010	03°	15	N286	20°	23	N162	31°		-//-	-//-
8	N260	11°	16	N030	10°	24	N000	06°		-//-	-//-

Table 4 : Measurements taken on the subhorizontal fractures on the station atMvog-Betsi
(position : N03°51'49,8'' ; E11°28'27,5'' ; H = 861 m)

N°	Azimuth	Dip	N°	Azimuth	Dip	N°	Azimuth	Dip	N°	Azimuth	Dip
1	N120	14°	9	N010	24°	17	N040	26°	25	N020	20°
2	N140	17°	10	N012	19°	18	N034	12°	26	N350	22°
3	N020	08°	11	N358	12°	19	N155	10°	27	N030	22°
4	N040	18°	12	N020	40°	20	N168	02°	28	N056	42°
5	N160	20°	13	N024	28°	21	N016	20°	29	N050	16°
6	N020	12°	14	N020	30°	22	N036	20°	30	N050	20°
7	N018	20°	15	N020	40°	23	N010	20°		-//-	-//-
8	N032	20°	16	N040	24°	24	N002	22°		-//-	-//-

Table 5 : Measurements taken on the subhorizontal fractures on the station at Nkolbisson
(position : N03°52'06,8'' ; E11°27'28,5'' ; H = 733 m) [25]

N°	Azimuth	Dip	N°	Azimuth	Dip	N°	Azimuth	Dip	N°	Azimuth	Dip
1	N080	18°	10	N073	26°	19	N102	28°	28	N078	32°
2	N070	26°	11	N073	16°	20	N106	22°	29	N072	18°
3	N040	22°	12	N068	17°	21	N098	19°	30	N072	22°
4	N068	29°	13	N072	16°	22	N075	21°	31	N078	25°
5	N082	53°	14	N082	12°	23	N078	18°	32	N100	32°
6	N071	33°	15	N080	10°	24	N054	22°	33	N070	17°
7	N063	28°	16	N078	18°	25	N050	22°		-//-	-//-
8	N083	25°	17	N089	22°	26	N042	22°		-//-	-//-
9	N084	28°	18	N082	27°	27	N100	24°		-//-	-//-

Table 6 : Measurements taken on the subhorizontal fractures on the station at Oliga
(position : N03°53'35,9'' ; E11°29'36,6'' ; H = 810 m) [25]

N°	Azimuth	Dip	N°	Azimuth	Dip	N°	Azimuth	Dip	N°	Azimuth	Dip
1	N174	15°	5	N170	14°	9	N198	20°	13	N187	18°
2	N180	23°	6	N190	18°	10	N182	24°	14	N181	17°
3	N202	24°	7	N202	08°	11	N170	18°	15	N186	13°
4	N190	27°	8	N170	18°	12	N160	20°	16	N182	16°

Table 7 : Measurements taken at the linear fractures of the station at Cité-verte
(position : N03°52'37,8'' ; E11°28'49,0'' ; H = 813 m)

N°	Strike	Apparent dip	N°	Strike	Apparent dip	N°	Strike	Apparent dip	N°	Strike	Apparent dip
1	N106E	82°	18	N100E	79°	35	N178E	84°	52	N086E	85°
2	N072E	88°	19	N090E	84°	36	N040E	88°	53	N088E	85°
3	N040E	90°	20	N052E	85°	37	N120E	88°	54	N000E	89°
4	N090E	86°	21	N042E	66°	38	N050E	86°	55	N090E	79°
5	N110E	80°	22	N088E	86°	39	N060E	86°	56	N090E	90°
6	N048E	90°	23	N088E	86°	40	N076E	90°	57	N070E	72°
7	N090E	90°	24	N089E	90°	41	N080E	90°	58	N180E	85°
8	N088E	90°	25	N090E	90°	42	N076E	87°	59	N016E	74°
9	N080E	82°	26	N018E	72°	43	N072E	90°	60	N150E	68°
10	N072E	76°	27	N130E	52	44	N084E	88°	61	N170E	76°
11	N010E	90°	28	N056E	87°	45	N086E	82°	62	N000E	78°

N°	Strike	Apparent dip	N°	Strike	Apparent dip	N°	Strike	Apparent dip	N°	Strike	Apparent dip
12	N080E	78°	29	N120E	60°	46	N086E	90°	63	N178E	82°
13	N068E	90°	30	N040E	74°	47	N072E	88°	64	N174E	84°
14	N090E	87°	31	N132E	54°	48	N154E	86°	65	N002E	90°
15	N020E	75°	32	N160E	70°	49	N004E	90°	66	N174E	88°
16	N035E	68°	33	N018E	77°	50	N176E	86°		-//-	-//-
17	N035E	68°	34	N140E	15°	51	N172E	87°		-//-	-//-

Table 8 : Measurements taken at the linear fractures of the station at Mvog-Betsi (position : N03°51'49,8'' ; E11°28'27,5'' ; H = 861 m) [25]

N°	Strike	Apparent dip	N°	Strike	Apparent dip	N°	Strike	Apparent dip	N°	Strike	Apparent dip
1	N130E	-//-	20	N130E	-//-	39	N040E	-//-	58	N150E	-//-
2	N140E	-//-	21	N126E	-//-	40	N122E	-//-	59	N150E	-//-
3	N122E	-//-	22	N122E	-//-	41	N138E	-//-	60	N140E	-//-
4	N138E	-//-	23	N138E	-//-	42	N138E	-//-	61	N152E	-//-
5	N112E	-//-	24	N112E	-//-	43	N120E	-//-	62	N121E	-//-
6	N112E	-//-	25	N112E	-//-	44	N144E	-//-	63	N040E	-//-
7	N120E	-//-	26	N120E	-//-	45	N120E	-//-	64	N180E	-//-
8	N030E	-//-	27	N120E	-//-	46	N031E	-//-	65	N160E	-//-
9	N030E	-//-	28	N120E	-//-	47	N033E	-//-	66	N136E	-//-
10	N030E	-//-	29	N040E	-//-	48	N030E	-//-	67	N120E	-//-
11	N130E	-//-	30	N042E	-//-	49	N130E	-//-	68	N045E	-//-
12	N122E	-//-	31	N122E	-//-	50	N122E	-//-	69	N040E	-//-
13	N122E	-//-	32	N130E	-//-	51	N130E	-//-	70	N035E	-//-
14	N130E	-//-	33	N140E	-//-	52	N078E	-//-	71	N140E	-//-
15	N065E	-//-	34	N140E	-//-	53	N124E	-//-	72	N130E	-//-
16	N128E	-//-	35	N138E	-//-	54	N030E	-//-	73	N130E	-//-
17	N150E	-//-	36	N150E	-//-	55	N150E	-//-		-//-	-//-
18	N180E	-//-	37	N156E	-//-	56	N125E	-//-		-//-	-//-
19	N152E	-//-	38	N155E	-//-	57	N160E	-//-		-//-	-//-

Table 9 : Measurements taken at the linear fractures of the station at Nkolbisson (position : N03°52'06,8'' ; E11°27'28,5'' ; H = 733 m) [25]

N°	Strike	Apparent dip	N°	Strike	Apparent dip	N°	Strike	Apparent dip	N°	Strike	Apparent dip
1	N006E	-//-	22	N172E	68°	43	N124E	-//-	64	N144E	-//-
2	N084E	-//-	23	N148E	-//-	44	N000E	-//-	65	N010E	-//-
3	N086E	-//-	24	N130E	-//-	45	N126E	-//-	66	N124E	-//-
4	N082E	-//-	25	N132E	-//-	46	N002E	-//-	67	N006E	-//-
5	N160E	-//-	26	N120E	-//-	47	N144E	-//-	68	N012E	-//-
6	N120E	-//-	27	N136E	-//-	48	N132E	-//-	69	N130E	-//-
7	N022E	-//-	28	N132E	-//-	49	N124E	-//-	70	N010E	-//-
8	N018E	-//-	29	N026E	-//-	50	N132E	-//-	71	N096E	-//-
9	N008E	-//-	30	N126E	-//-	51	N016E	-//-	72	N008E	-//-
10	N008E	-//-	31	N002E	-//-	52	N130E	-//-	73	N140E	-//-
11	N030E	-//-	32	N006E	-//-	53	N020E	-//-	74	N120E	-//-
12	N128E	-//-	33	N140E	-//-	54	N122E	-//-	75	N006E	-//-
13	N012E	-//-	34	N150E	-//-	55	N138E	-//-	76	N132E	-//-
14	N150E	-//-	35	N138E	-//-	56	N016E	-//-	77	N026E	-//-
15	N084E	-//-	36	N024E	-//-	57	N016E	-//-	78	N024E	-//-
16	N086E	-//-	37	N002E	-//-	58	N126E	-//-	79	N014E	-//-
17	N138E	-//-	38	N004E	-//-	59	N122E	-//-	80	N120E	-//-
18	N124E	-//-	39	N084E	-//-	60	N150E	-//-	81	N129E	-//-
19	N000E	-//-	40	N144E	-//-	61	N018E	-//-		-//-	-//-
20	N152E	-//-	41	N132E	-//-	62	N012E	-//-		-//-	-//-
21	N100E	-//-	42	N120E	-//-	63	N144E	-//-		-//-	-//-

Table 10 : Measurements taken at the linear fractures of the station at Oliga (position : N03°53'35,9'' ; E11°29'36,6'' ; H = 810 m) [25]

N°	Strike	Apparent dip	N°	Strike	Apparent dip	N°	Strike	Apparent dip	N°	Strike	Apparent dip
1	N100E	-//-	9	N036E	-//-	17	N040E	-//-	24	N098E	-//-
2	N092E	-//-	10	N100E	-//-	18	N120E	-//-	25	N028E	-//-
3	N028E	-//-	11	N114E	-//-	19	N020E	-//-	26	N092E	-//-
4	N086E	-//-	12	N038E	-//-	20	N091E	-//-	27	N040E	-//-
5	N040E	-//-	13	N028E	-//-	21	N150E	-//-	28	N124E	-//-
6	N036E	-//-	14	N036E	-//-	22	N096E	-//-	29	N036E	-//-
7	N070E	-//-	15	N036E	-//-	23	N036E	-//-	30	N020E	-//-
8	N056E	-//-	16	N086E	-//-		-//-	-//-		-//-	-//-

Table 11 : Stereogram and rosette of the planar and linear fractures [25]

Planar fractures of the Cité-Verte site	Linear fractures of the Cité-Verte site
Planar fractures of the Mvog-Betsi site	Linear fractures of the Mvog-Betsi site
Planar fractures of the Nkolbisson site	Linear fractures of the Nkolbisson site
Planar fractures of the Oliga site	Linear fractures of the Oliga site
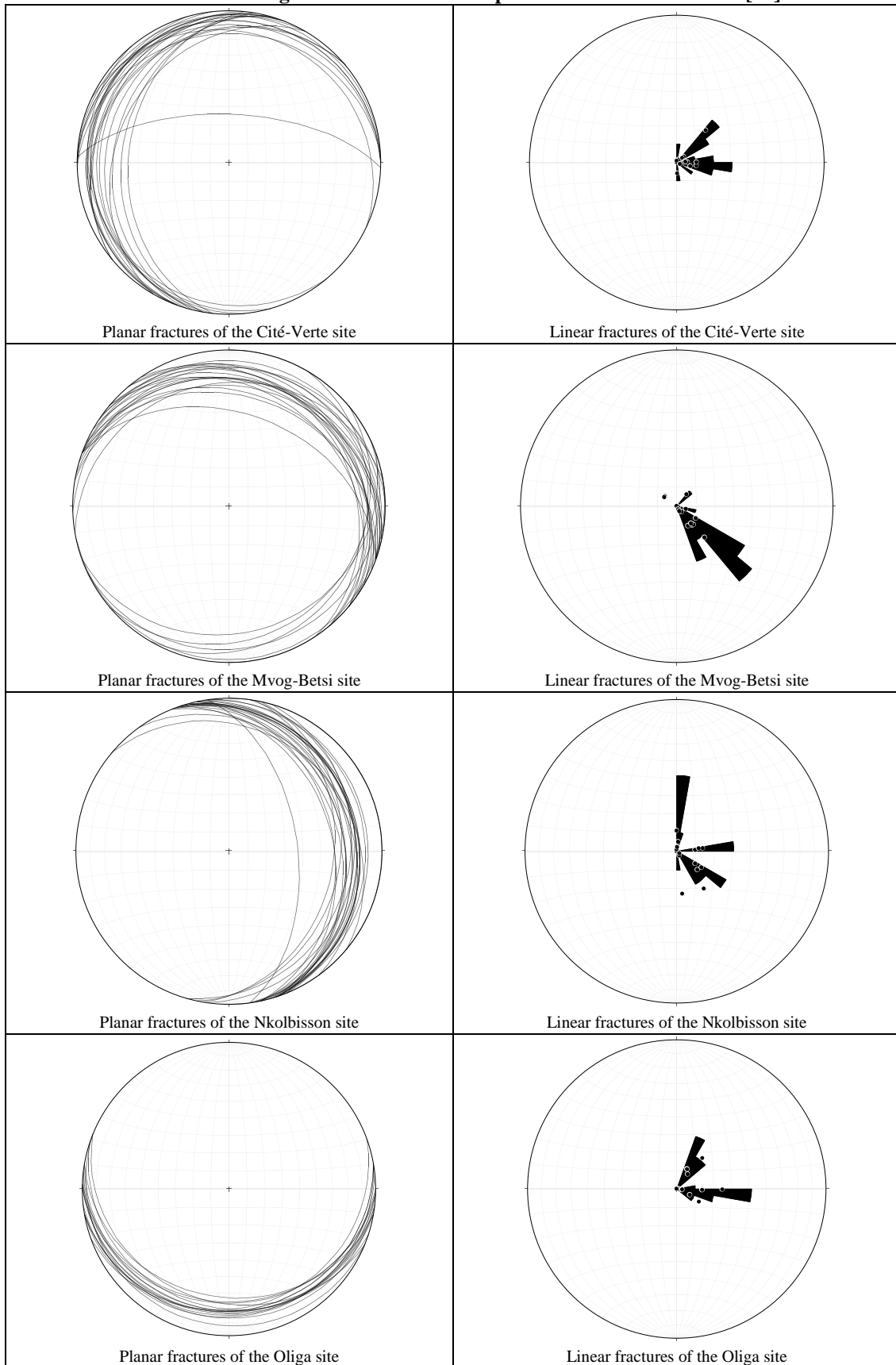
Table 12 : Orientation of constraint and deformation at certain measurements stations [25]
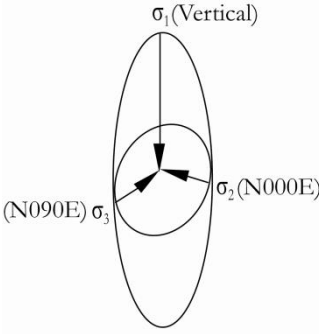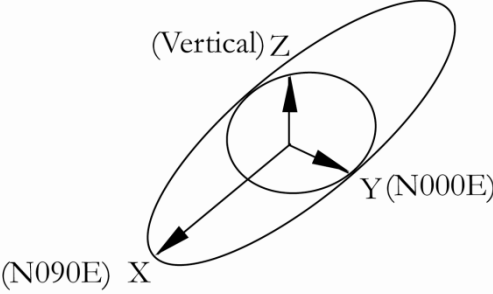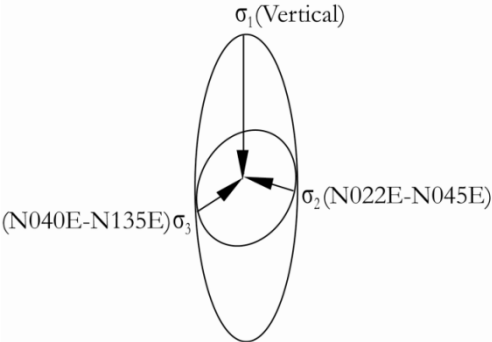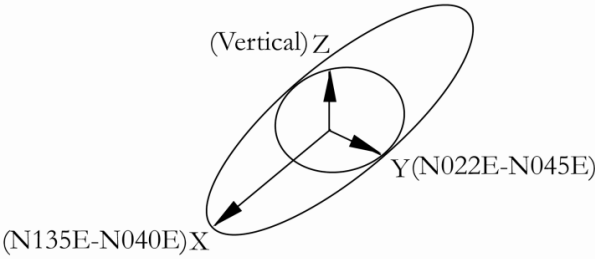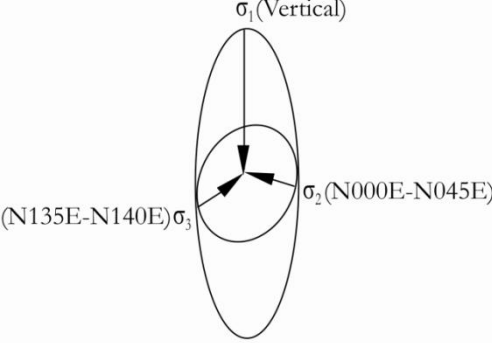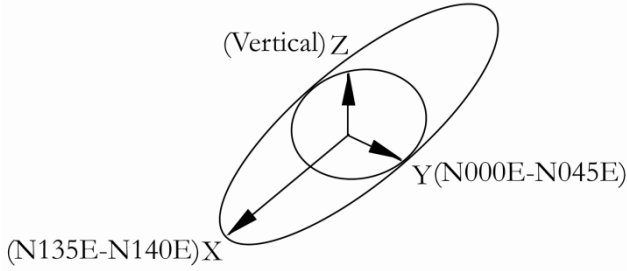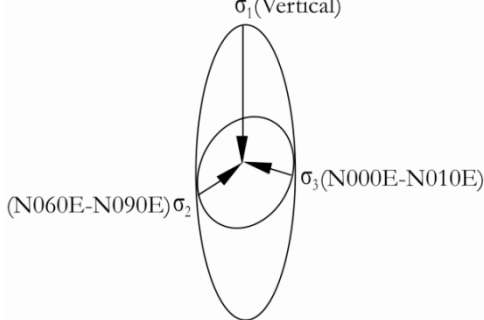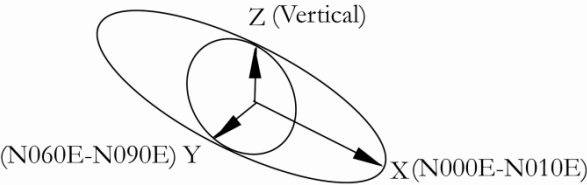
Constraint ellipsoid	Deformation ellipsoid
At the measurement station of Cité-verte	
At the measurement station of Mvog-Betsi	
At the measurement station of Nkolbisson	
At the measurement station of Oliga	

Figure 5 : Grid following the cracks on the outcrop of Cité-verte (N03°52'37,8'' ; E11°28'49,0'' ; H = 813 m) [25]

Figure 6 : Grid following the cracks on the outcrop of Mvog-Betsi (N03°51'49,8'' ; E11°28'27,5'' ; H = 861 m) [25]

Figure 7 : Grid following the cracks on the outcrop of Nkolbisson (N03°52'06,8'' ; E11°27'28,5'' ; H = 733 m) [25]

Figure 8 : Grid following the cracks on the outcrop of Oliga (N03°53'35,9'' ; E11°29'36,6'' ; H = 810 m) [25]

Table13 : Average spacing at the measurement station of Cité-verte [25]

E_x (m)	Nombre	E_y (m)	Nombre	E_z (m)	nombre
0,80	5	0,50	15	0,30	7
1,00	5	0,80	10	0,45	8
1,30	20	1,50	15	0,60	15
2,00	10	2,00	1	0,80	10
3,00	2	4,00	5	1,00	19
Total	42	Total	46	Total	59
E_{xm}	1,45 m	E_{ym}	1,30 m	E_{zm}	0,71 m

1.2.2.2.   Intense fracturation at the megascopic scale

Fractures revealed by hydrographic and orographic alignments of N-S orientation, orographic alignments of E-W orientation, and faults of intermediary orientation between NW-SE and SW-NE directions (*Fig. 9, 10 and 11*).

The Yaounde region is broken into blocks [**14**]. This division creates two great families of faults (N-S and E-W) and an intermediary family (NW-SE et SW-NE).This distribution leads to predict the regional shearing (*Fig. 12*).
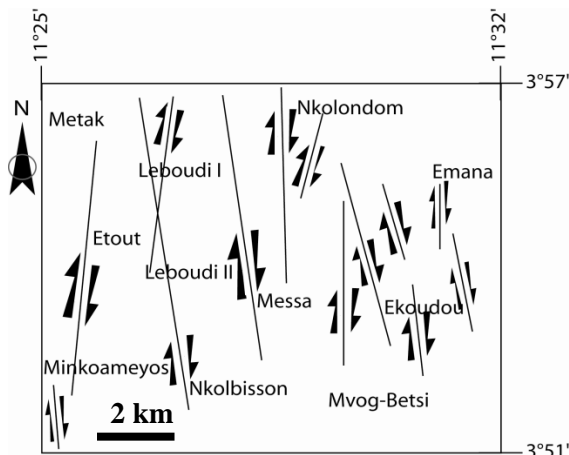
Figure 9 : Map of N-S fractures regrouping the hydrographic and orographic alignments or lineations [14]
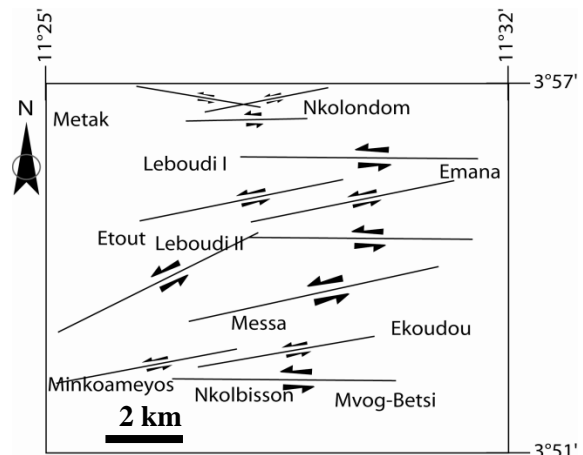
Figure 10 : Map of E-W fractures regrouping the hydrographic and orographic alignments or lineations [14]
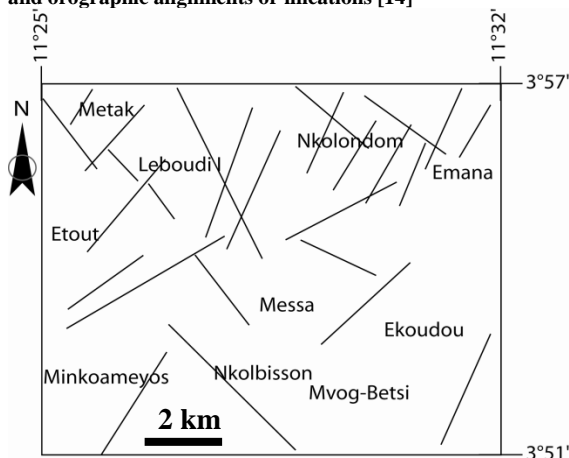
Figure 11 : Map of intermediate oriented faults of between NW-SE and SW-NE directions [14]
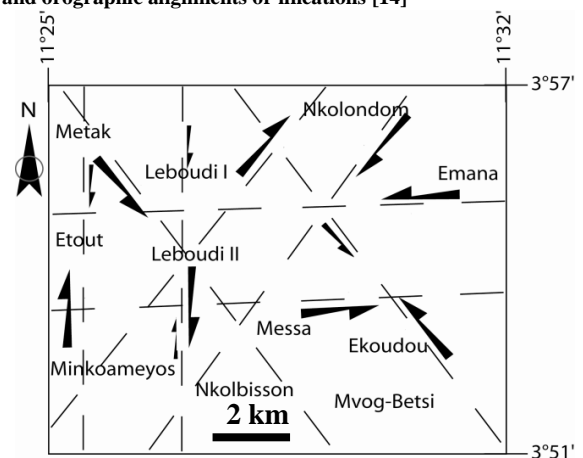
Figure 12 : Map of the shear corridors of the Yaounde region [14]

1.2.2.3.   Quasi-symmetrical folds at mesoscopic and megascopic scales

Syn-metamorphic ductile deformation phases that have affected the sedimentary and plutonic protoliths within the Yaounde region have shaped the geomorphological model into domes and bassins (*Fig. 13*). Thus, between the valleys, are found the hills in "half oranges" of some hundreds of metres in height [**7**].
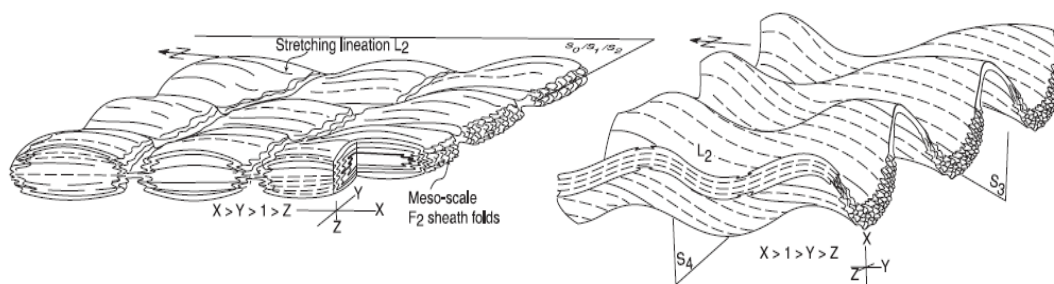
Figure 13 : Quasi-symmetrical folds support the geomorphological model of domes and valleys [26]

1.2.2.4.   Slump phenomenon

The links between the different geomorphological units are oriented following the major axis of orogenesis (*Fig. 14*).

The revealed morphologies by the geological cross-sections leads us to be able to locate in parts and others domes, slumping structures, in two considered opposite directions; there appears some stages, that is a succession of structures that affect all of the units (*Sheet. 1 and 2*). That is summarized in a succession of blocks of variable sizes producing a "horst and graben" relief of which the fault planes are normal, clearly visible above 800 m which are generally the upthrown sections (*Sheet. 3*).
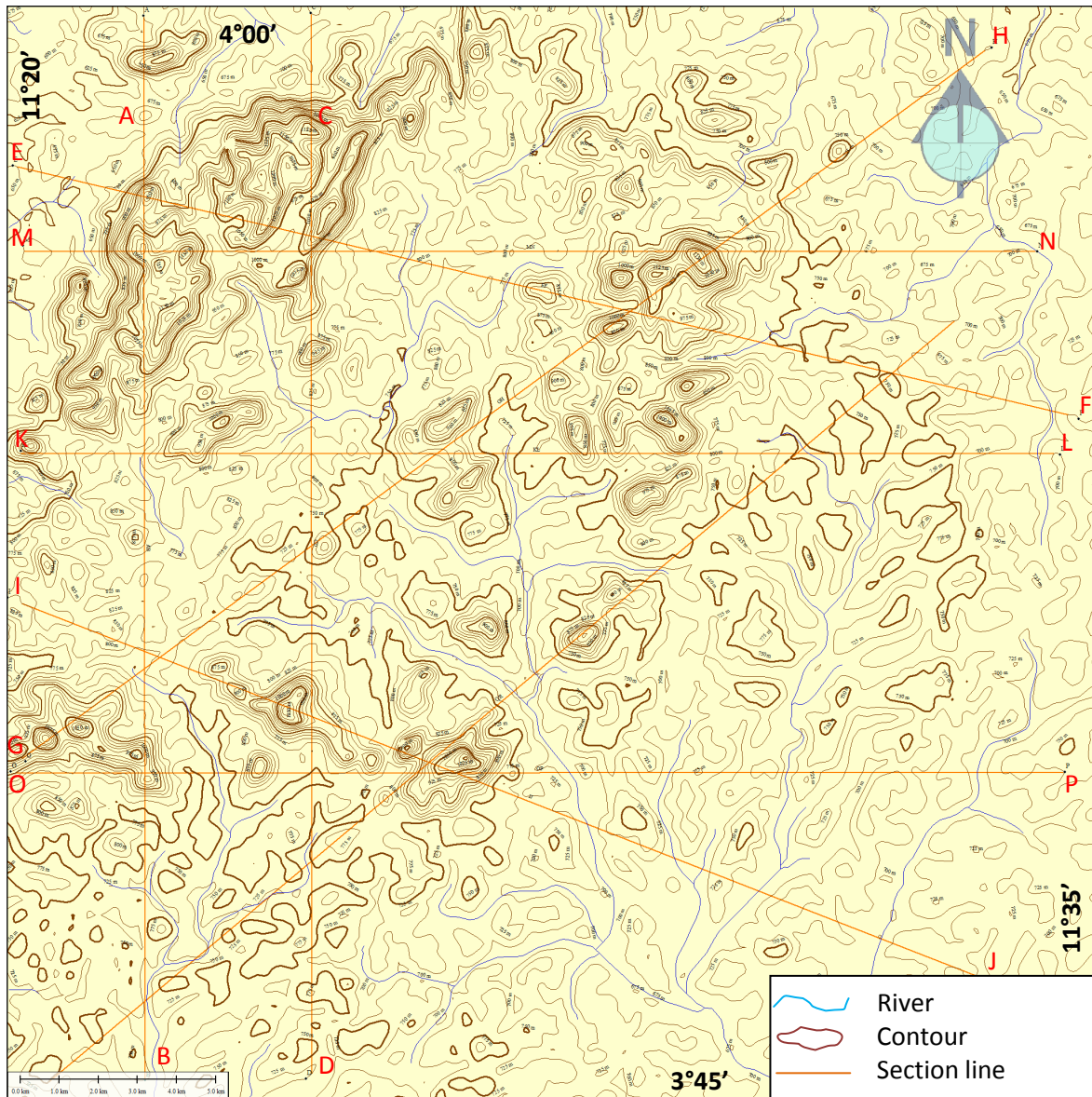
Figure 14 : Map of section lines across the highs reliefs of the study area

Profile along the section line AB
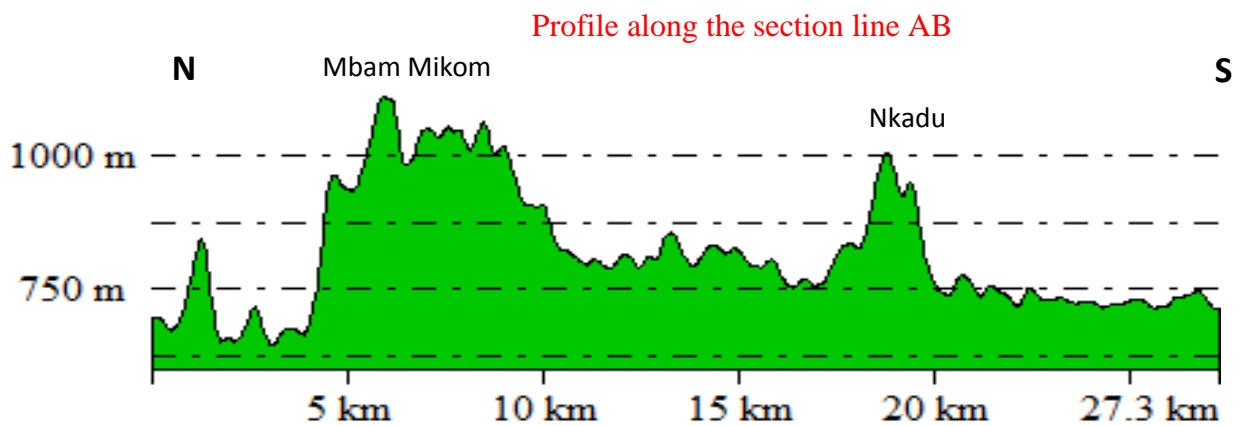
Profile along the section line CD
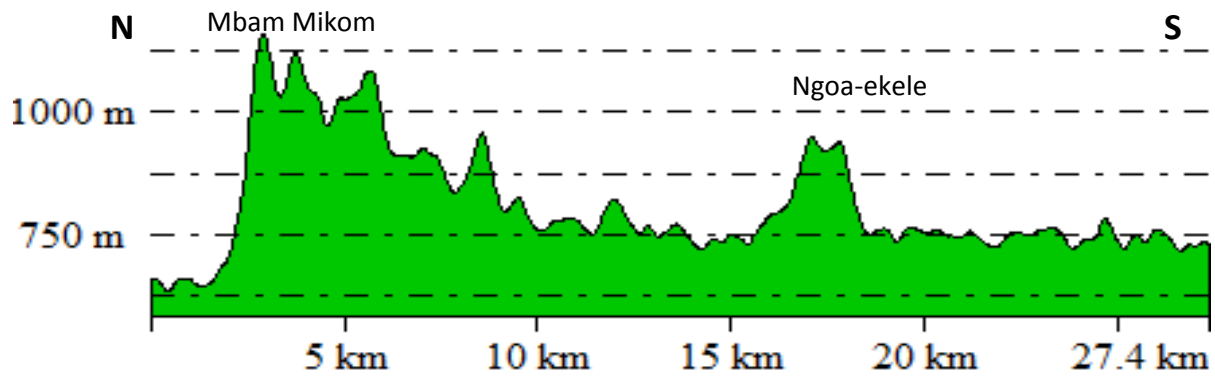
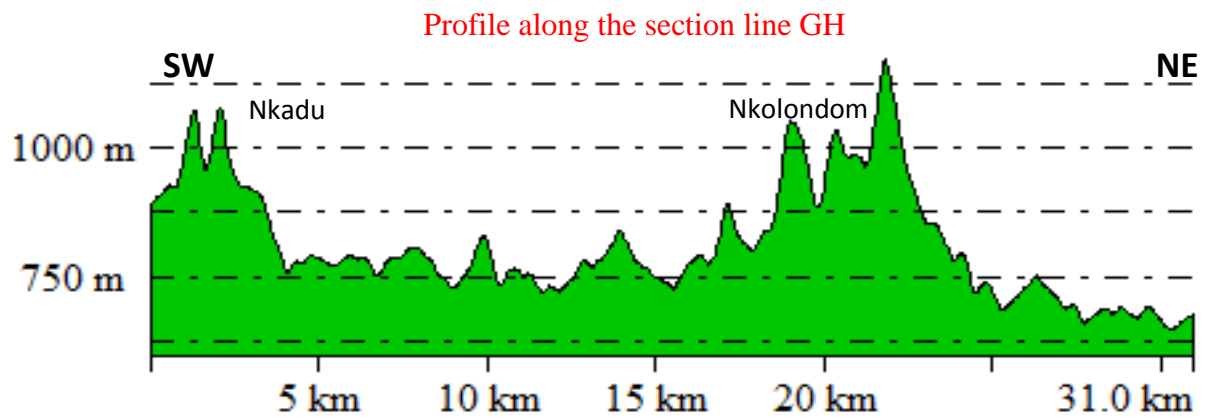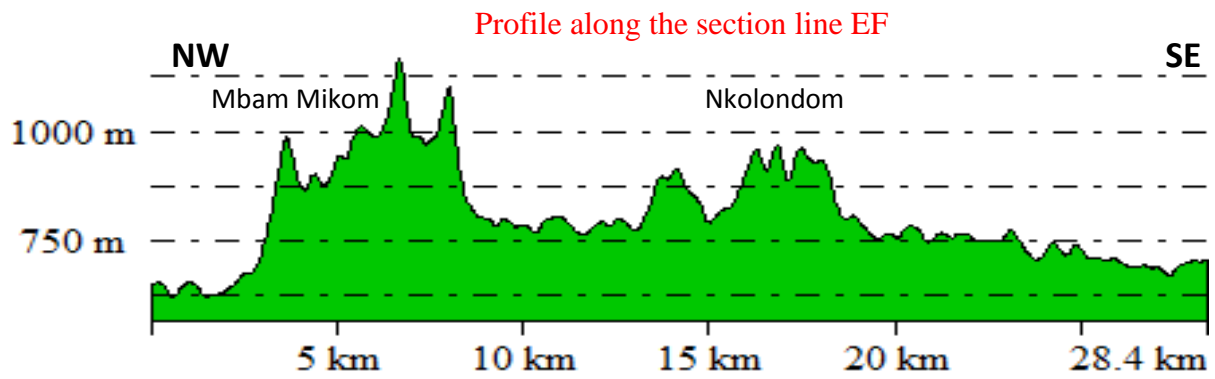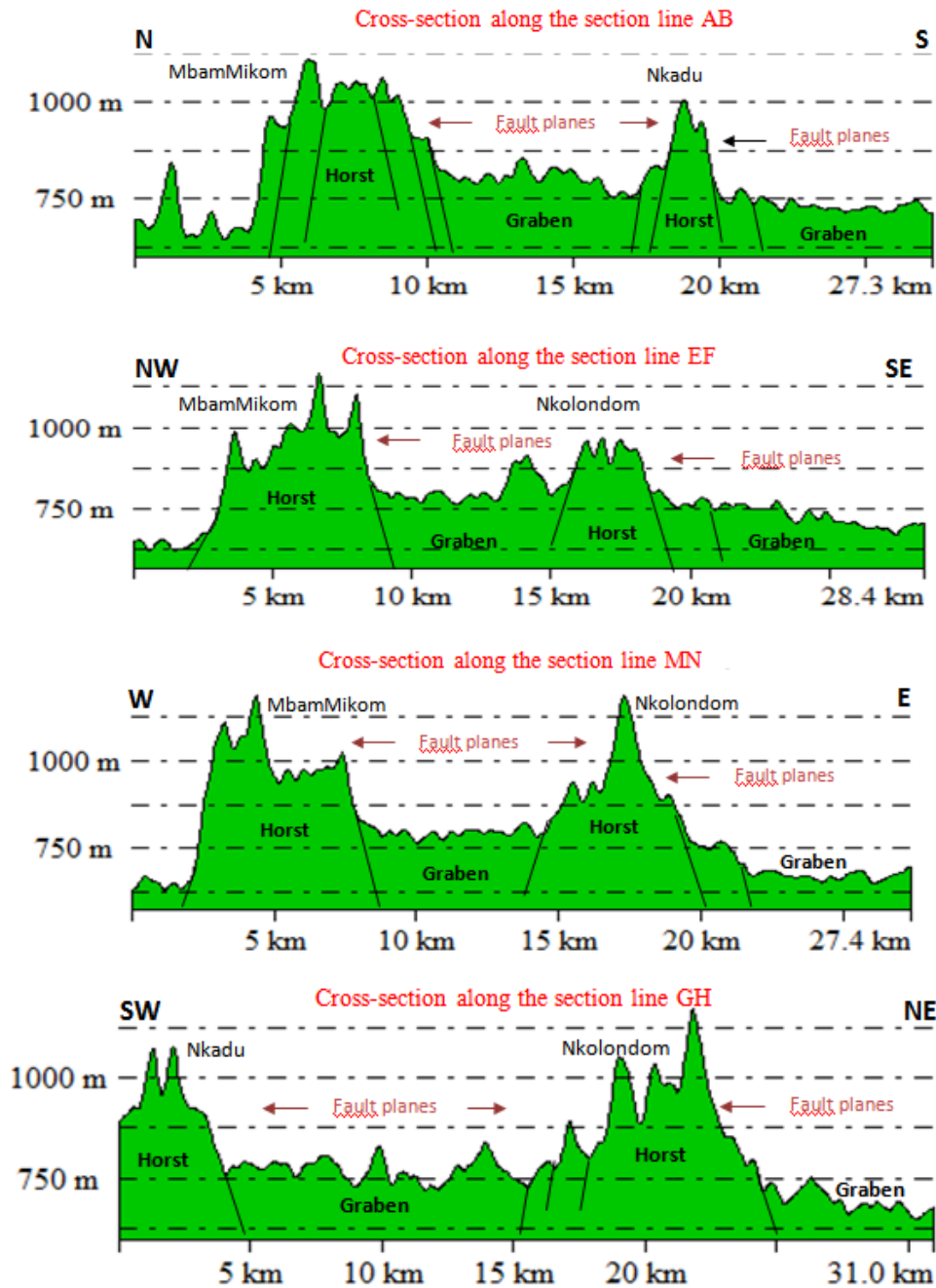Profile along the section line MN
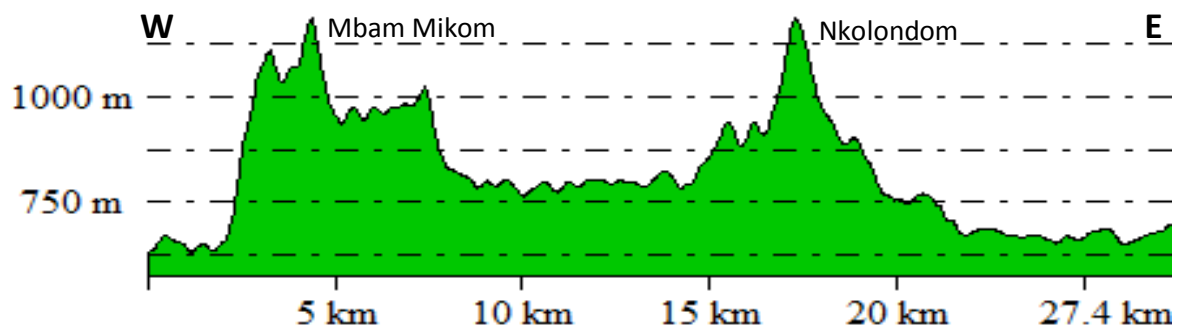
Profile along the section line KL
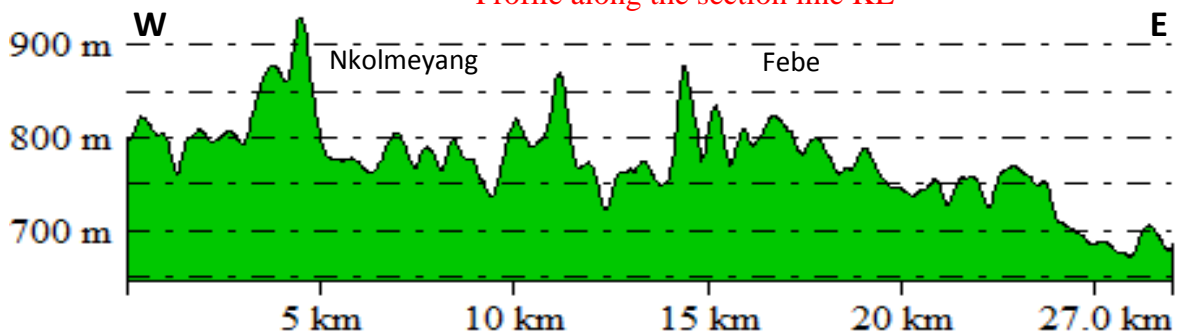
Profile along the section line OP
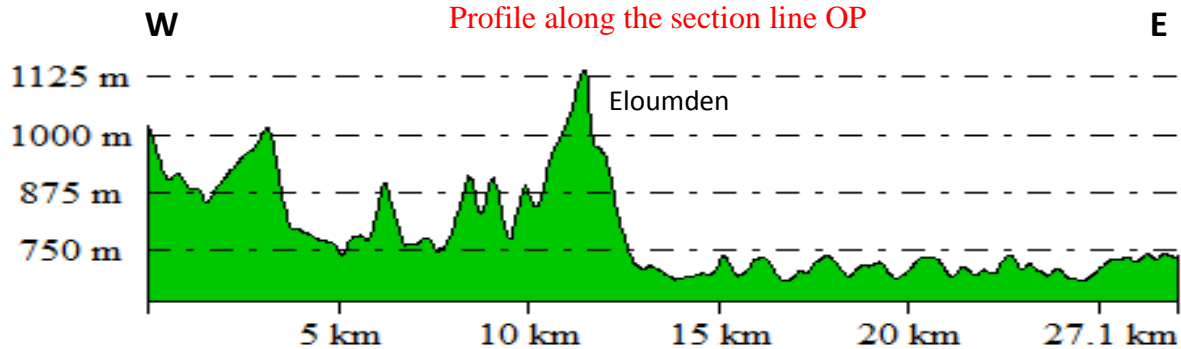
Sheet 15 : Oriented N-S and E-W profiles
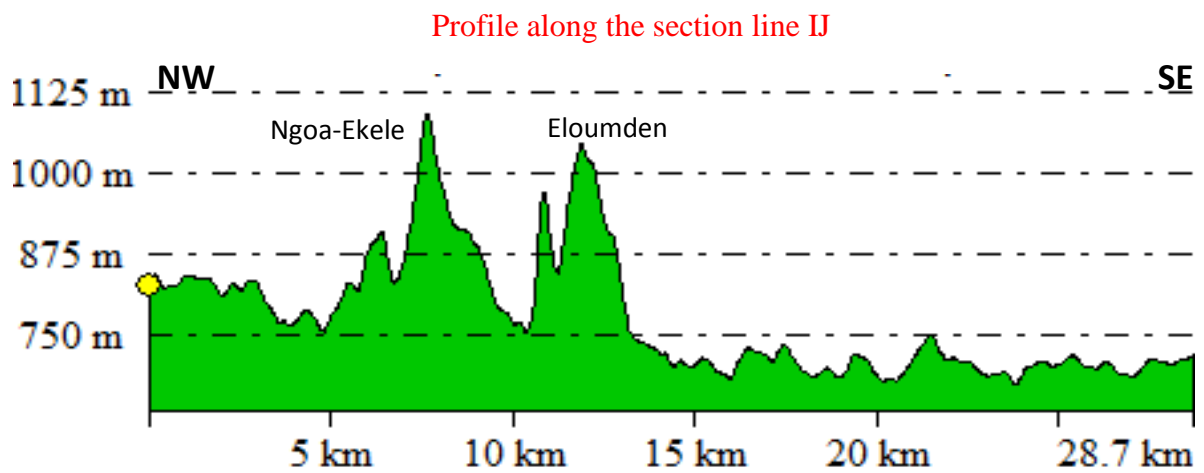
Sheet 2 : Oriented NW-SE and SW-NE profiles

Sheet 3 : Geological cross-sections showing tectonic slumping ; stages showing "horst and graben" (note the abundance of normal faults in which the upthrown sections are seen in the form of fault planes)

1.2.3.   Distribution of soils
•   Varieties of soils
The soils of the Yaounde region are well differentiated at mid-slope (*Fig. 15 and 16*) and less evolved at the hill tops (*Fig. 17*). From 800 m, they are encrusted with blocks.
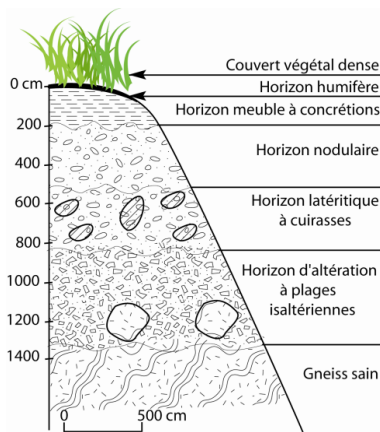
Figure 165 : Soil profile on the foot of slope and at the middle slope : thick and encrusted of rocky blocks [25]
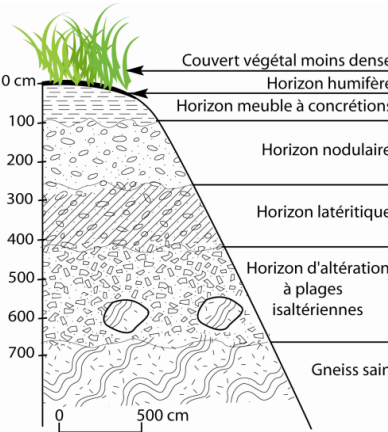
Figure 176 : Soil profile at the middle slope : less thicker and encrusted with rocky blocks [25]
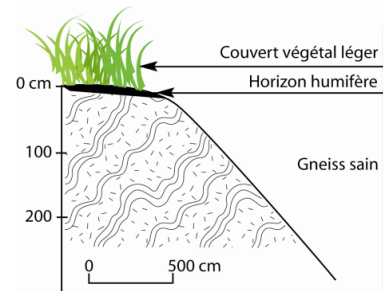
Figure 187 : Soil profile on the summit : very thin and less evolved [25]

- Distribution of the soil varieties

The distribution is subconcentric around the summits of outcrops and covers lithic less evolved soils or red ferralitic soils. Towards the flanks and the valleys appear typical ferralitic soils, a bit thick and at times encrusted of rocky blocs (*Photo 11a and 11b*).

Photo 10 : Road cut T_2 (extremity (a) and medium sector (b) of the cutting)

- Physical and chemical properties of soils

The physico-chemical properties of the soils in the study zone are those of typical ferralitic soils : Liquidity Limit (WL) is about 50% and 70% ; Plasticity Limit(WP) is gotten between 20% and 40% ; Plasticity Index (Ip) is between 20% and 40% and the Saturation point (Sr) attains 85% during adverse conditions **[27]**.

1.2.4. Distribution of the parent rock

- Variety of mother rock

The katazone of Yaounde region is characterised by the presence of light petrographic types (metasediments) and dark petrographic types (metaplutonites) and granitic intrusions dated from Mesoproterozoic to Nesoproterozoic **[26]**. Their outcrops follow a subconcentric distribution around the summits.

At a macroscopic scale, the light petrographic type is compact and shows a compositional banding characterised by the alternation of light and dark bands. Quartz represents 30% to 40% in the composition of the rock **[28]** and its grains vary from 0.2 to 0.5 cm. plagioclases represent 20% to 30% in the composition of the rock **[28]** and their sizes vary between 0.3 cm to 0.5 cm. muscovite is present in the form of very thin sheets of 0.02 à 0.07 cm. Biotite represents 5% to 10% in the composition of the rock **[28]** and having size varying from 0.2 to 0.9 mm. the rock is spotted of pink grains of garnet, of varying sizes from 0.1 cm to 0.3 cm and of Kyanite of varying sizes between 0.1 cm and 0.2 cm. Garnet and Kyanite represent 15% to 20% and 2,5% in the composition of the rock **[28]**. Certain minerals such as Graphite, Rutile, Zircon and Monazite are accessory (*Sheet 4*).

At the macroscopic scale the dark petrographic type is compact and shows also a compositional banding characterised by the alternation of light and dark bands. Quartz makes 30% to 40% of the rocks composition **[28]** and vary from 0.1 to 0.5 cm. Plagioclases represent 40% to 50% in the composition of the rock **[28]** and their

sizes vary between 0.1 to 0.5 cm. Biotite represents 5%to 10% of the composition of the rock **[28]**, its grains varying from 0.2 to 0.9 mm. Muscovite and Pyrite exist in the form of very thin sheets of 0.2 à 0.7 mm and represents 2%to 5% in the composition of the rock **[28]**. The rock is mixed with brick red grains of Garnets, of sizes varying between 0.1 cm and 0.2 cm and sheets of Pyrites of sizes varying between 0.1 cm and 0.2 cm. Garnet represents 10%to 20% in the composition of the rock **[28]**. Accessory minerals in the rock are Graphite, Rutile, Zircon and Monazite (***Sheet 5***).

- Ancient and present Karst phenomenon at the heart of the rocks

Numerous forms comparable to those encountered in the karstic model is observed at the core of the gneiss of the Yaounde region (***Fig. 18, 19, 20, 21, 22 and 23***). These forms are either present and formed under atmospheric air under the effects of rain water, either too old and initially formed in a wet milieu ; their formation and disposition being strongly controled by structural characters of the rocks **[29]**.

The structuration of gneiss shows a foliation and subhorizontal shearing planes that facilitates the formation of sheet joints. The vertical and horizontal of rain water that leads to the enlargement of the structural joints by dissolution, with consequence of the facilitation of rolling of the large blocks of rocks on the flanks of the hills. Very large blocks are formed which are decametric in size, which usually roll down the flanks of the hills due to earthquake tremors.
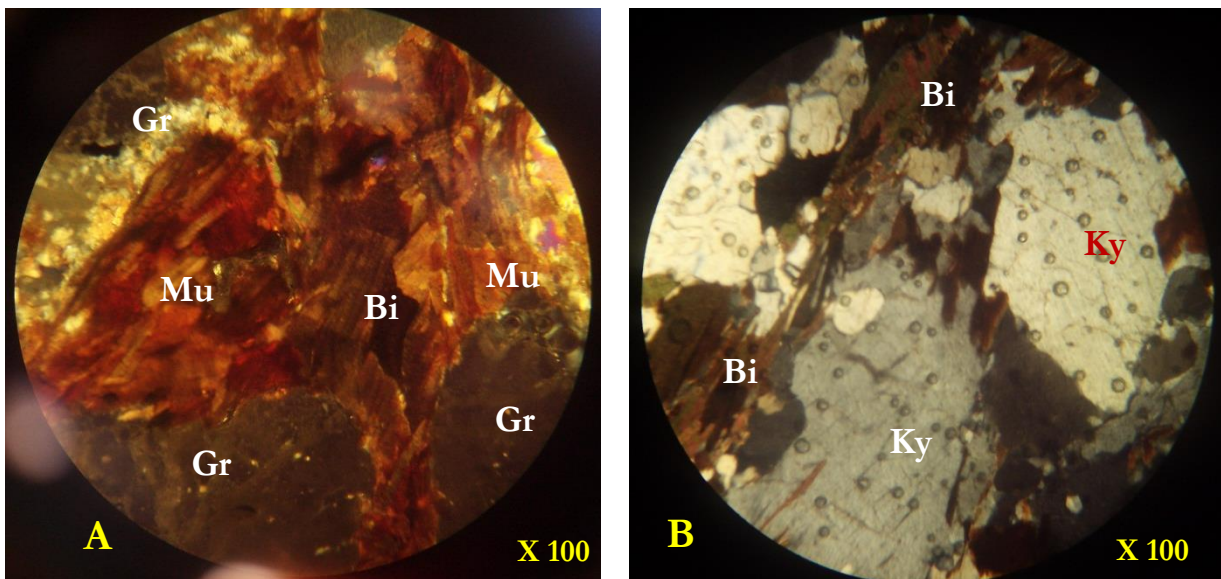
Sheet 4 : Microscopic organisation of garnet and kyanite gneiss at the Cité-verte site
(Gr = garnet, Mu = muscovite, Qtz = quartz, Bi = biotite, Ky = Kyanite) [25]
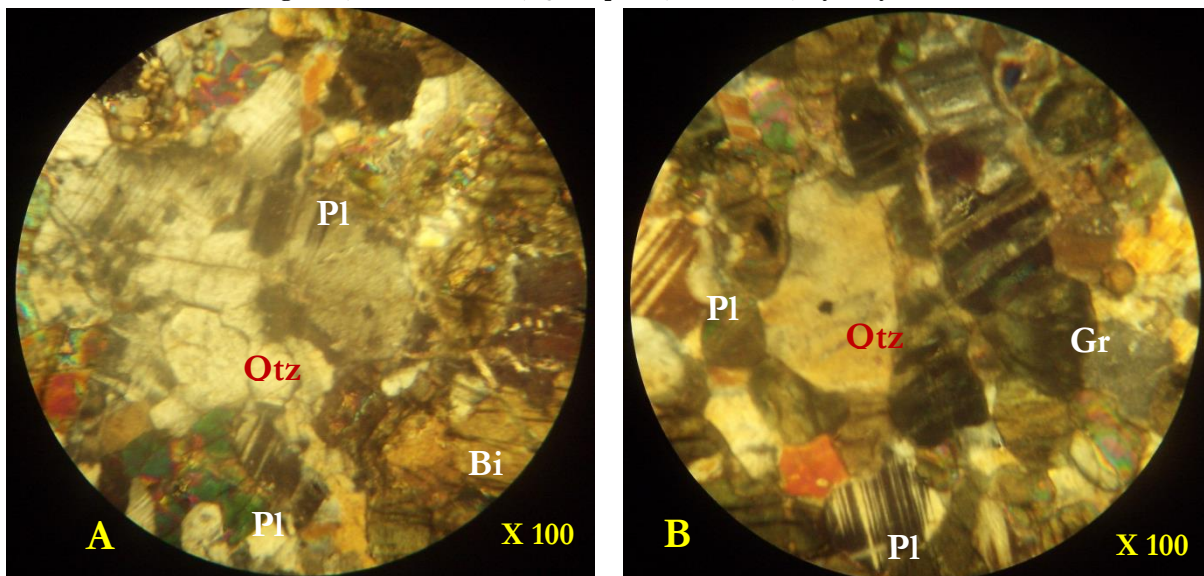
Sheet 5 : Microscopic organisation of garnet and plagioclase gneiss at the Nkolnyada site
(Gr = garnet, Qtz = quartz, Bi = biotite, Pl = plagioclase, Ky = kyanite) [25]

Figure 19 : Garnet-Kyanite gneiss (take note of the disorganised banding by migmatisation)

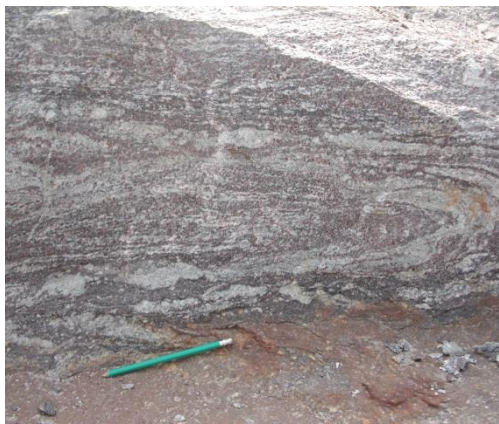**Figure 20 : Garnet-Plagioclase gneiss (take note of the inclusions)**

Figure 21 : Garnet-Kyanite gneiss

Figure 22 : Garnet-Plagioclase gneiss

Figure 23 : Weathered and fractured gneiss (saprolith) below a thin soil at Nkolnyada (Tsinga) site

Figure 243 : Wall alveolus on the Mvog-Betsi hill [29]

1.3.   Vectorisation of primary information maps

The vectorisation of master lines of isoaltitudes in Mapinfo® from the numerical model of the topographical map has help to realise the map of altitude values.

The extraction of major fractures from hydrographical and orographical lineaments has help to the realisation of the deep fracture map.

The vectorisation of relative data to the distribution of soil varieties in Mapinfo® from the map of soil varieties in southern Cameroon and the field data has also helped to the realization of soil distribution map.

The vectorisation of relative data to the distribution of the parent rock varieties in Mapinfo® from the field data has helped to realize the map of the distribution of parent rock varieties.

1.4.   Synchronisation of primary information maps

The simultaneous treatment of the different thematic maps of observation and analysis (***Fig. 24***) in Mapinfo® by the crossing or superposition of vectorised maps (***Fig. 25, 26, 27 and 28***) has helped to realise a map of the considered landslide and rock fall hazard study.
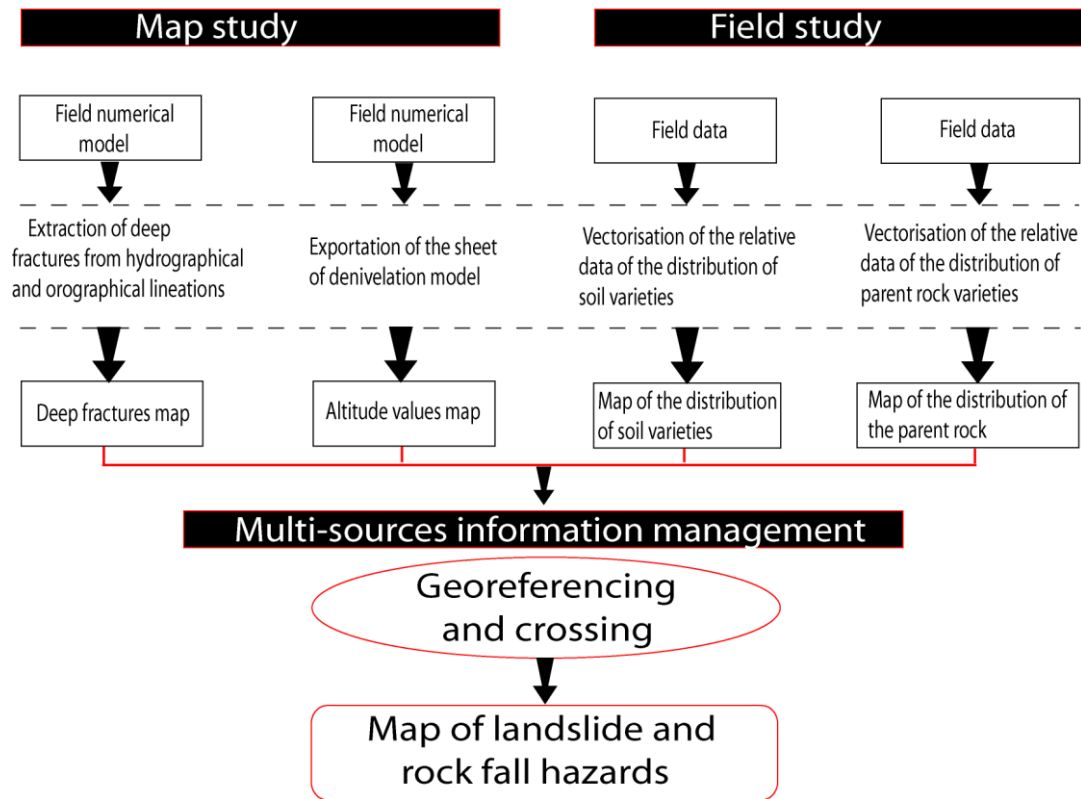

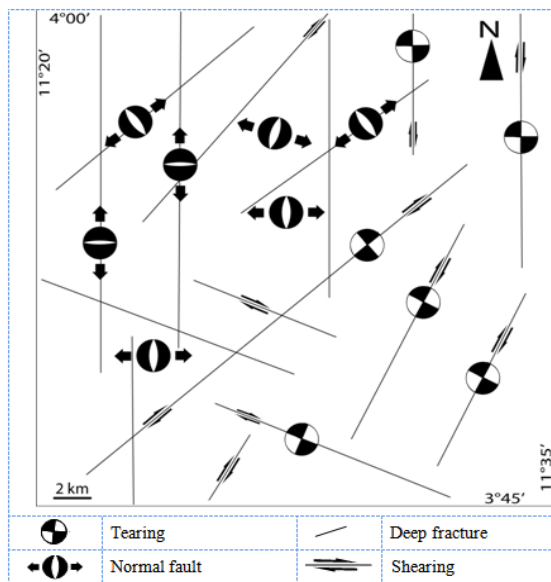**Figure 254 : Itinerary of the crossing of the vectorised maps**
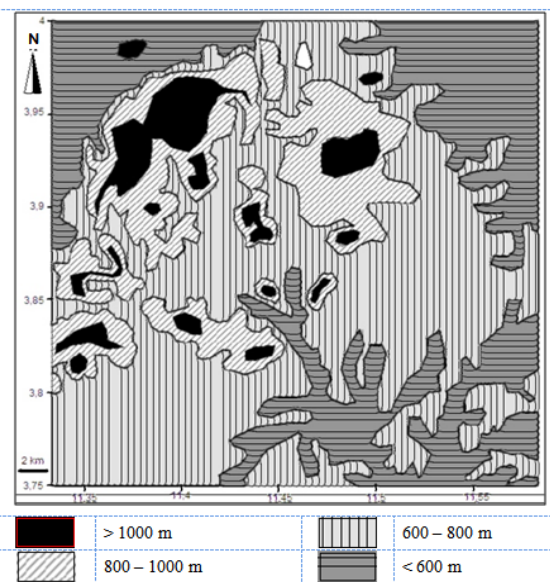

| | Tearing | | Deep fracture | | > 1000 m | | 600 – 800 m |
| | Normal fault | | Shearing | | 800 – 1000 m | | < 600 m |

Figure 265 : Map of deep fractures   **Figure 276 : Map of altitude contours values [25]**
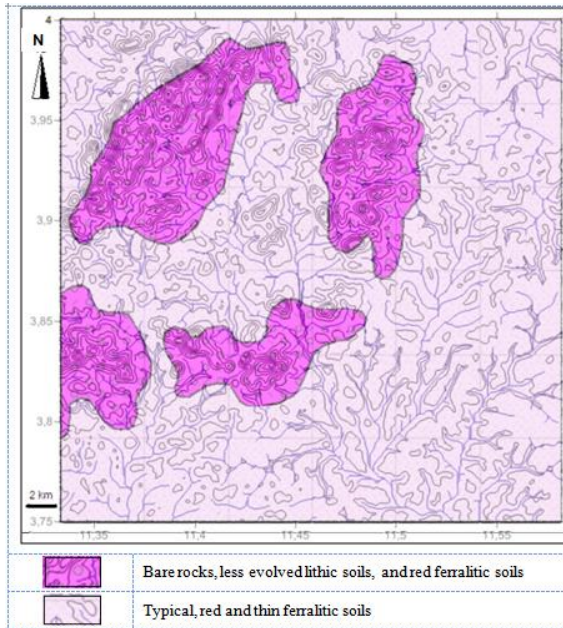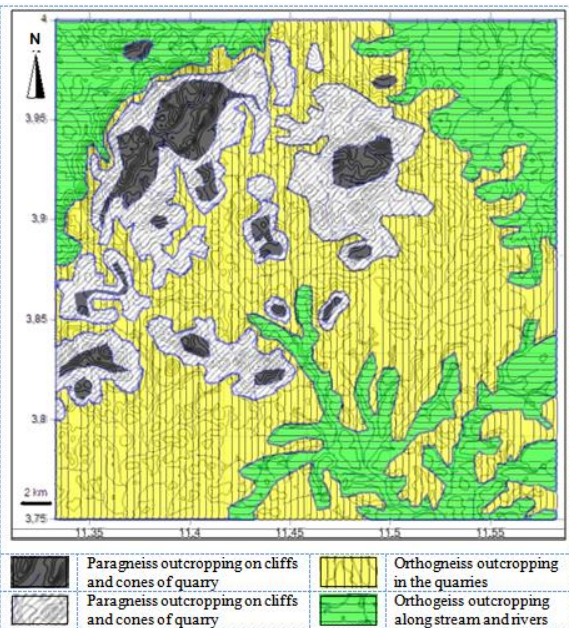
Figure 287 : Map of the soil varieties distribution [25]

Figure 298 : Map of the distribution of parent rock varieties [25]

II. RESULTS AND DISCUSSION

3.1. Map from the crossing of multi-sources information

The crossing of deep fractures map, contour values map, map of the distribution of soil varieties and the map of the distribution of parent rocks varieties (*Fig. 29*) has helped to obtain a detailed map on the landslide and rock fall hazard in the North-West section of Yaounde region Where the hazard is "very high" in three major lineation oriented SSW-NNE and E-W ; and "high to average" in two lineation oriented WSW-ENE (*Fig. 30*).
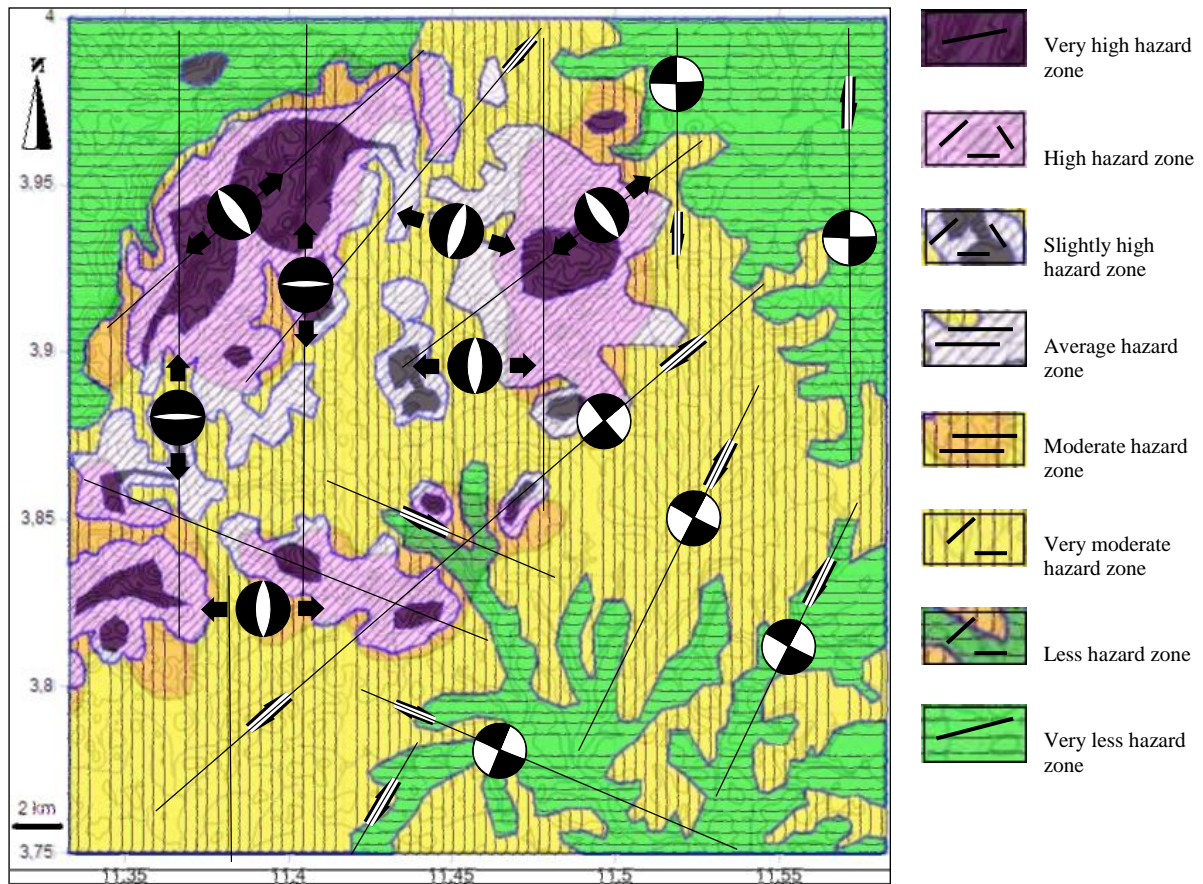

Figure 309: Zoned map of the landslide and rock fall hazard [25], modified
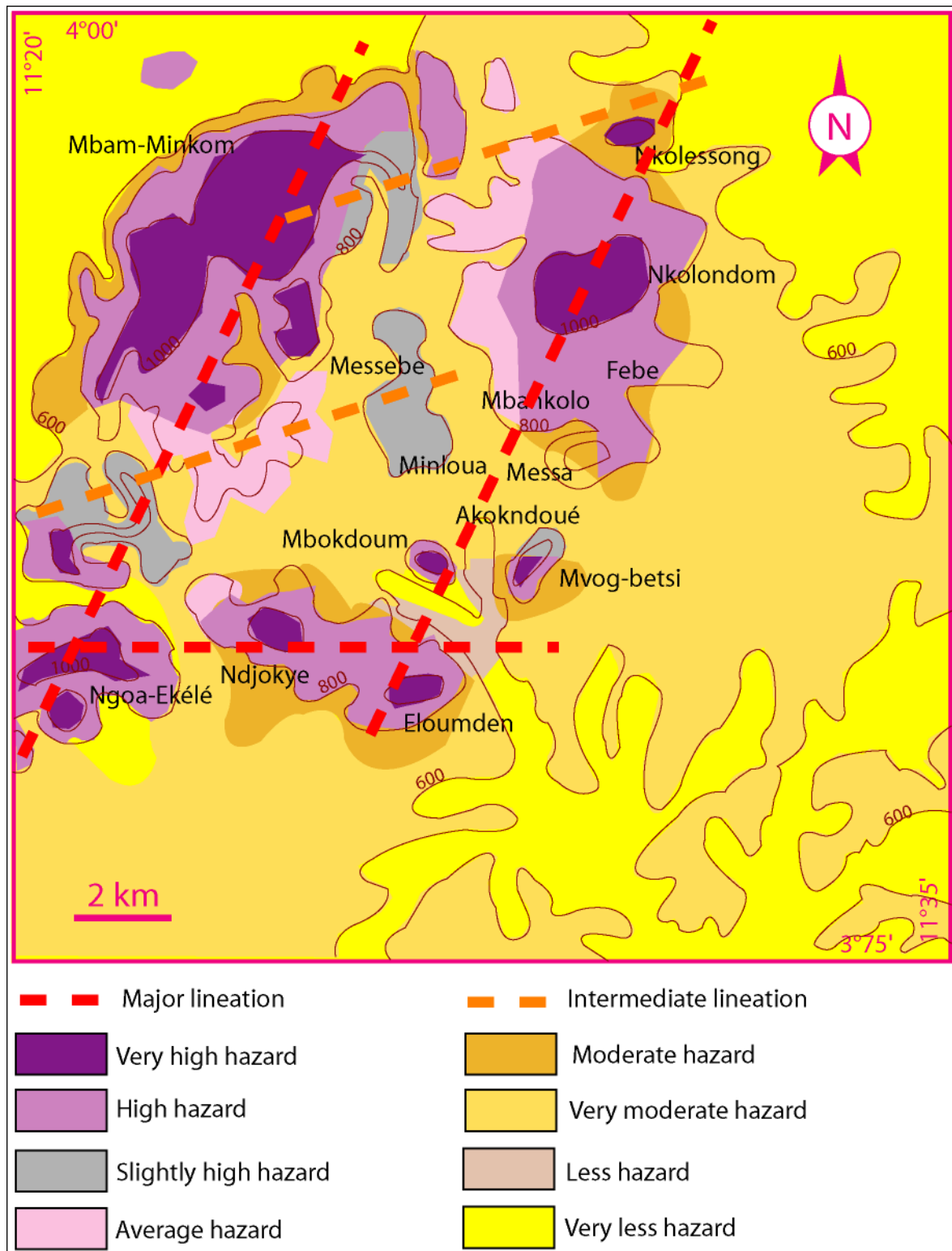
Figure 30 : Synthesis map for landslide and rock fall hazards

3.2.   Interpretation

The interpretation used is based on the hypothesis that within the zone of study four factors were necessary and enough to constitute the landslide and rock fall hazards : the altitude, the fracturation of the bedrock, soils varieties and varieties of the parent rock. In this context, a lot of decisions had been used **[30]** to cross in the form of logical combination or the said parametres before obtaining a classification (***Fig. 31 and Table 14***).
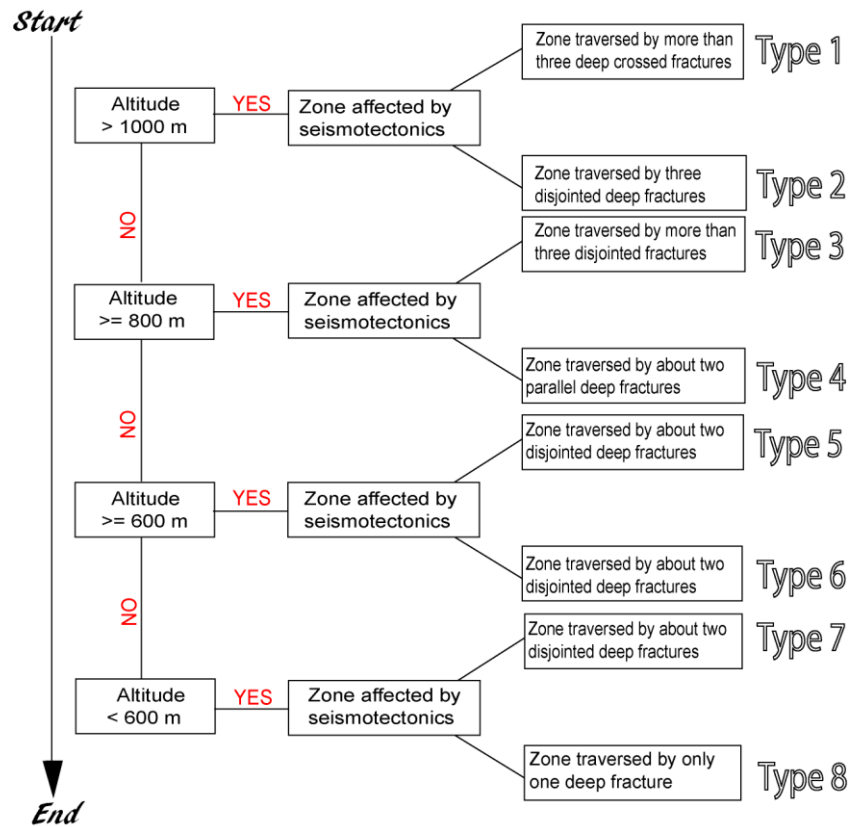
Figure 31 31: Decision tree [25], modified by the new arrangement of hazard factors

Table 14 : Translation of types in magnitude of hazards

Types	magnitudes	Types	Magnitudes
Type 1	Very high hazard zone	Type 5	Moderate hazard zone
Type 2	High hazard zone	Type 6	Very moderate hazard zone
Type 3	Slightly high hazard zone	Type 7	Less hazard zone
Type 4	Average hazard zone	Type 8	Very less hazard zone

III. CONCLUSION

The concatenation of field, library and laboratory data and the synchronization of multiple sources of information using a GIS enabled the generation of a thematic map that demonstrates that the morpho-tectonic state of the North-West sector of the region of Yaounde is the predominant factor of the sensibility of the slopes to the landslide and rock fall.

Zonal map reveals a "very high hazard" in three major lineation oriented towards SSW-NNE and E-W; and a "high to average" hazard in two intermediate lineation oriented WSW-ENE

BIBLIOGRAPHY

[1]. M. Lassere and D. Soba, Migmatisation d'âge panafricain au sein des formations camerounaises appartenant à la zone mobile de l'Afrique Centrale, *Compte Ren du Somm. Soc. Géol. Fr*., 2, 1979, 64-68.
[2]. B. Bessole and R. Trompette, *Géologie de l'Afrique. La chaîne panafricaine « zone mobile d'Afrique Centrale (partie sud) et zone mobile soudanaise »*, Mém. BRGM, Orléans, 92, 1980, 394p.
[3]. J.-P. Nzenti, Pétrogenèse des migmatites de Yaoundé (Cameroun) : éléments pour un modèle géodynamique de la chaine panafricaine nord-équatoriale,Thèse Univ.,Nancy I, 1987, 147p.
[4]. J.-P. Nzenti, P. Barbey, J. Macaudiere,D. Soba,Origin and evolution of the late precambrian high grade Yaounde gneisses (Cameroon), *Precambrian Research, 38*, 1998, 91-109.
[5]. J. L. Poidevin, Tectonique panafricaine à la bordure nord du craton congolais : l'orogenèse des « Oubanguides », *12ᵗʰ Coll. Afr. Geol. Brussels (Abstract)*, 1983,75p.
[6]. R. Trompette, *Geology of Western Gondwana : (2000 – 500 Ma)*,(A.A. Belkeema, Roterdam, 1994).
[7]. C. Moreau and R. T. Ghogomu,Résultats préliminaires à l'étude structurale des migmatites de Yaoundé,in Ann. Fac. Sci. Terre, série IV, tome 1, n°1, 1982, 105-111.
[8]. H. Mvondo, J. Essono, J. MvondoOndoa, J. Q. YeneAtangana, Comment on "U-Pb dating of plutonic rocks involved in the nappe tectonic in southern Cameroon: Consequence for the Pan-African orogenic evolution of the central African fold belt" by Toteu et al. (Journal of African Earth Sciences 44 (2006) 479-493), *Journal of African Earth Sciences, 48*, 2007a, 49-52.
[9]. J. Mvondo Ondoa, *Caractérisation des évènements tectoniques dans le domaine Sud de la chaine panafricaine au Cameroun : styles tectoniques et géochronologie des séries de Yaoundé et Bafia*, Thèse Doc. Ph/D, Univ. Ydé I, 2009, 189p.
[10]. S. F. Toteu, W. R. Van Schmus, J. Penaye,J. B. Nyobe, U-Pb and Sm-Nd evidence for Eburnian and Pan-African high grade metamorphism in cratonic rocks of Southern Cameroon, *Precambrian. Research, 67*, 1994, 321-347.

[11]. S. Owona, M. Tichomirowa, L. Ratschbacher, J. MvondoOndoa, D. Youmen, J. Pfänder, F. M. Tchoua, P. Affaton, G. E. Ekodeck, New igneous zircon Pb/Pb and metamorphic Rb/Sr ages in the Yaounde Group (Cameroun, Central Africa) : implications for the Central African fold belt evolution close to the Congo Craton, *International Journal of Earth Sciences, 101*(7), 2012, 1689-1703.

[12]. M. M. Enama, *Contribution à l'étude pétrostructurale et à la cartographie des métamorphites dans le Nord de Yaoundé*, Mém. Maît., Fac. Sci., Univ. Ydé, 1998, 95p.

[13]. J. Niyonkuru, *Contribution à l'étude de la fracturation de la région de Yaoundé et ses environs*, Mém. Maît. Fac. Sci. Univ. Ydé I, 2001.

[14]. F. Mvondo Owono, *Nouvelle approche de la déformation progressive du contexte fragile à Yaoundé et ses environs*, Mém. DEA, Fac. Sci. Univ. Ydé I, 2001, 60p.

[15]. R. J. Assako Assako, Apport des systèmes d'information géographique dans l'analyse des risques d'inondation et glissement de terrain à Yaoundé, in De Bergier, *Villes du Sud et environnement*, (Châteauneuf de Grasse, 1997), 110-126.

[16]. D. Fekoua, *Anthropisation et risques environnementaux sur les collines de Yaoundé*, Mém. Master pro. Cresa-Bois. Univ. Dsc., 2010, 88p.

[17]. Ministère du Développement Urbain et de l'Habitat and Communauté Urbaine de Yaoundé, *Yaoundé 2020 : Plan directeur d'urbanisme* (Communauté Urbaine de Yaoundé, 2008), 120p.

[18]. R. Bissaya, *Analyse géologique de la sensibilité des versants aux glissements de terrain et aux éboulements en zone de hauts reliefs : cas du secteur Nord-Ouest de la région de Yaoundé*, Mém. Master, Fac. Sci. Univ. Ydé I, 2011, 144p.

[19]. Onguene Mala, *Différenciation pédologique dans la région de Yaoundé (Cameroun) : transformation d'un sol ferrallitique rouge en sol à horizon jaune et relation avec l'évolution du modélé*, Thèse Doc. Univ. Paris VI, 1993, 253p.

[20]. W. Oloumou, *Caractérisation morphologique et minéralogique des couvertures pédologiques des hauts reliefs de la région de Yaoundé*, Mém. DIPES II ENS, Univ. Ydé I, 1996, 61p.

[21]. Institut National de Cartographie- *Yaoundé 3d et Yaoundé 3c*, 1986.

[22]. W. B. Ambeh, J. D. Fairhead, D. J. Francis, J. M. Nnange, S. Djallo, Seismicity of the Mont Cameroon Region, West Africa, *Journal of African and the Middle East Earth Sciences, 9*(1), 1989, 1-7.

[23]. I. K. NJILAH, Geochemistry and Petrogenesis of Tertiary Quaternary volcanic rocks from the Oku-Ndu Area, NW Cameroon, PhD Thesis, Univ. of Leeds, UK, 1991, 345 p.

[24]. M. Ruhland, Méthodes d'étude de la fracturation naturelle des roches associées à divers modèles structuraux, Bull. Sc. Géol. Strasbourg, 1973, 26-27.

[25]. R. Bissaya, R. T. Ghogomu, A. Moundi, B. Njom, N. S. Kanouo, The use of geological data and the management of multiple information sources for the analysis of landslide and rockfall in the North-West section of the region of Yaounde, *Afriquesciences, 10*(3), 2014, 113-133.

[26]. H. Mvondo, S. Owona, J. Mvondo Ondoa, J. Essono,Tectonic evolution of the Yaoundé segment of the Neoproterozoïc Central African Orogenic Belt in southern Cameroon, *Canadian Journal of Earth Sciences, 44*, 2007b, 433-444.

[27]. Laboratoire National de Génie Civil, Dossiers Y. 87-2908/EF 1286, Y.86-2857/EF 1262, Y.78-1557/EF 368, Cameroun.

[28]. J.-P. Nzenti and S. M. Eno Belinga, Géologie de la région de Yaoundé et ses environs in excursions géologiques dans le sud du Cameroun, *12ème Conférence Internationale de la Société Géologique Africaine*, Univ. Ydé, 2001, 19-30.

[29]. .-P Vicat, H. Mvondo, L. Willems, A. Pouclet, Fossil and present-time karstic phenomena in silico-aluminous metamorphic formations of the Pan-African nappe of Yaoundé (South-Cameroon), *C. R. Geosciense, 334*, 2002, 545-550.

[30]. O. Cerdan, Y. Le Bissonnais, V. Souchere, C. King, V. Antoni, N. Surdyk, I. Dubus, D. Anouays, J. F. Desprats,*Guide méthodologique pour un zonage départemental de l'érosion des sols*, Rapp. n°3 BRGM /RP.55104-FR, 2006, 87p.